ISSN 0370-1972
Phys. Status Solidi B
249 · No. 6 June
1085–1300 (2012)

# physica status solidi b

www.pss-b.com

basic solid state physics

6
2012

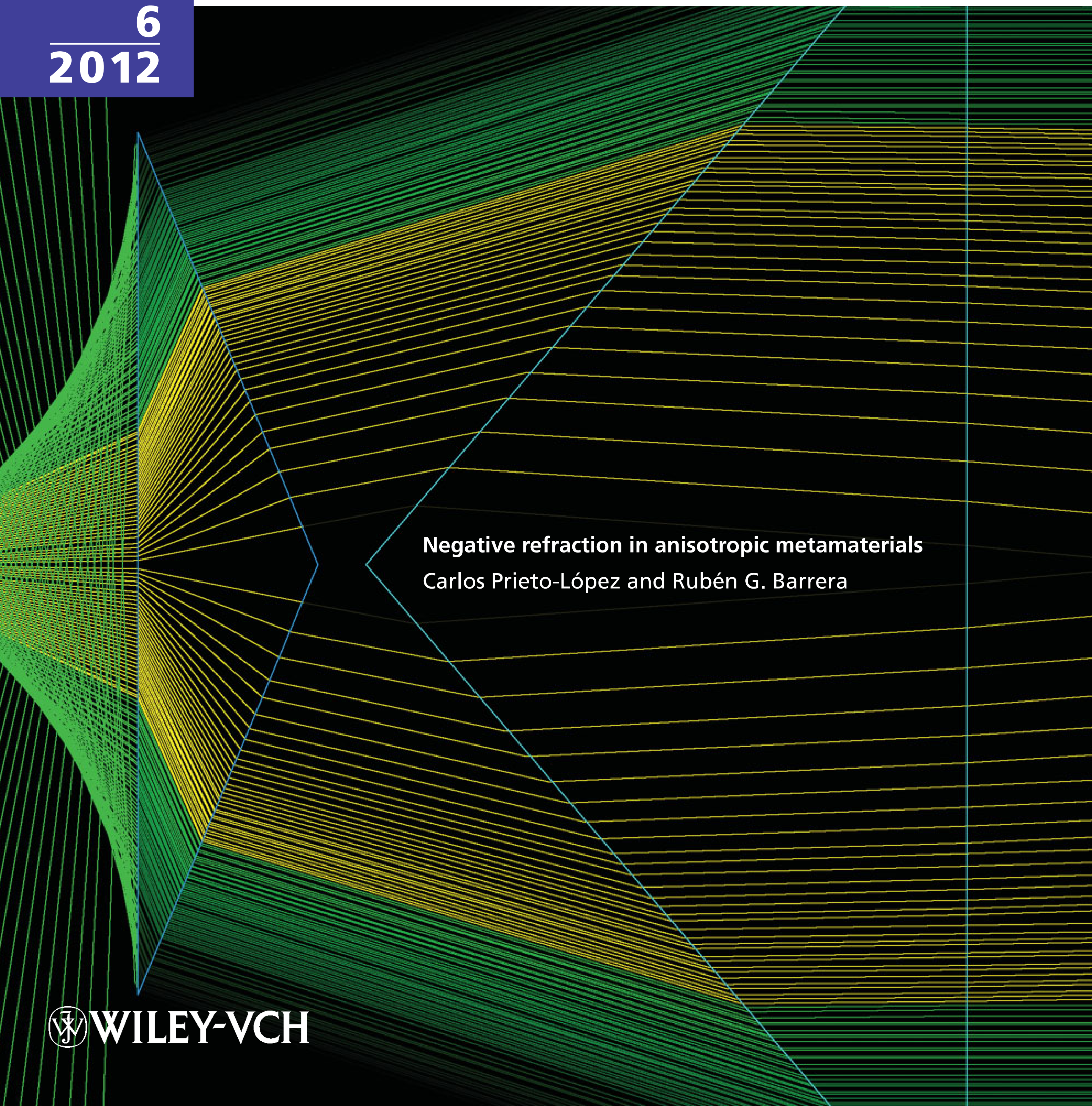

**Negative refraction in anisotropic metamaterials**

Carlos Prieto-López and Rubén G. Barrera

WILEY-VCH

physica status solidi

pss

www.pss-journals.com

reprint


WILEY-VCH

Phys. Status Solidi B **249**, No. 6, 1110–1118 (2012) / **DOI** 10.1002/pssb.201100747

physica status solidi b
www.pss-b.com
*basic solid state physics*

# Negative refraction in anisotropic metamaterials

**Carlos Prieto-López* and Rubén G. Barrera**

Instituto de Física, Universidad Nacional Autónoma de México, Apartado Postal 20-364, 01000 Distrito Federal, Mexico

Received 5 October 2011, revised 13 April 2012, accepted 15 April 2012
Published online 30 May 2012

**Keywords** anisotropic metamaterial, antireflective, collimator, negative refraction

* Corresponding author: e-mail caarlos@ciencias.unam.mx, Phone: +52-55-56554805, Fax: +52-55-56161535

In this paper we analyse the self-propagation of electromagnetic modes within an uniaxial non-absorbing metamaterial with anisotropic electric permittivity and anisotropic magnetic pemeability, for arbitrary values of the anisotropy ratios $\varepsilon_{\|}/\varepsilon_{\perp}$ and $\mu_{\|}/\mu_{\perp}$. We then solve the problem of refraction and reflection from a flat interface of this material when the interface is perpendicular to the optical axis. We establish the general conditions under which negative refraction occurs and study some properties of refraction, reflection and their potential applications.



**1 Introduction** The study of the optical properties of anisotropic materials has a history of over a century, and one of the main areas in these studies has been the optical properties of crystalline matter. The electromagnetic response of a wide variety of materials in the linear regime, is usually described exclusively in terms of an electric permittivity tensor $\overleftrightarrow{\varepsilon}$, since at high frequencies the magnetic response of common matter is extremely weak [1]. Also, since the actual anisotropy in the tensorial components of real crystals is not too large, cases in which the values of these components yield unrealistic anisotropies have not been considered either interesting or useful. But the work of Veselago [2] and the further development of metamaterials [3] have shown that values for the electromagnetic response that once were considered unrealistic can be actually attained. This is the case of isotropic metamaterials designed to have, within a definite frequency band, an effective magnetic permeability and an effective electric permittivity, both negative, which yield interesting phenomena like negative refraction, and gave rise to new concepts like left-handed materials. Analysis of the conditions for negative refraction in metamaterials with uniaxial, non-dissipative electric permittivity $\overleftrightarrow{\varepsilon}$ and magnetic permeability $\overleftrightarrow{\mu}$ have been made previously [4, 5] and the advantages for the design of these metamaterials have also been discussed. Here we present a further study of the properties of these materials and show some unexplored possibilities on their behaviour.

We explore the consequences of having a wide range of values for the four different components of $\overleftrightarrow{\varepsilon}$ and $\overleftrightarrow{\mu}$, and we establish the general conditions for negative refraction. We find, in contrast to the isotropic case, that negative refraction is possible when only one of the tensorial components, $\varepsilon_{\perp}$ or $\mu_{\perp}$, becomes negative. Also, for some range of values of the tensorial components of $\overleftrightarrow{\varepsilon}$ and $\overleftrightarrow{\mu}$, we find an interesting behaviour of the reflection and transmission amplitudes as a function of the angle of incidence and of the angle of refraction. All these results will allow to exploit anisotropic metamaterials. The structure of this paper is as follows: in Section 2 we study the electromagnetic properties of the bulk. In Section 3 we set an interface between vacuum and an anisotropic material and derive the laws of refraction as well as some of their properties. In Section 4 we study the reflection amplitudes of this interface, and in Section 5 we propose a design for a collimator of diffuse light using the optical properties studied previously.

**2 Electromagnetic modes** We will consider an uniaxial anisotropic material whose response tensors are given by

$$\overleftrightarrow{\mu} = \mu_{\|}\left(\mathbf{e}_x\mathbf{e}_x + \mathbf{e}_y\mathbf{e}_y\right) + \mu_{\perp}\mathbf{e}_z\mathbf{e}_z, \tag{1}$$

$$\overleftrightarrow{\varepsilon} = \varepsilon_{\|}\left(\mathbf{e}_x\mathbf{e}_x + \mathbf{e}_y\mathbf{e}_y\right) + \varepsilon_{\perp}\mathbf{e}_z\mathbf{e}_z, \tag{2}$$

in which $\mathbf{e}_i$ denotes a unit vector along the $i$th cartesian axis. We have aligned the $z$ axis with the optical axis. The system is excited by an electromagnetic wave oscillating within a frequency window in which the material is non-absorbing, thus the tensorial components of $\overleftrightarrow{\varepsilon}$ and $\overleftrightarrow{\mu}$ can be regarded as real quantities. As we can see, this material is characterised in terms of only four scalar quantities: $\varepsilon_\parallel$, $\varepsilon_\perp$, $\mu_\parallel$ and $\mu_\perp$.

In order to derive the dispersion relation of the electromagnetic modes in this system, first we write $\overleftrightarrow{\mu}$ and $\overleftrightarrow{\varepsilon}$ in terms of the anisotropy parameters: $a_m = \mu_\parallel/\mu_\perp$ and $a_e = \varepsilon_\parallel/\varepsilon_\perp$, as

$$\overleftrightarrow{\mu} = \mu_\parallel\left(\overleftrightarrow{I} + \left(\frac{1}{a_m} - 1\right)\mathbf{e}_z\mathbf{e}_z\right), \quad (3)$$

$$\overleftrightarrow{\varepsilon} = \varepsilon_\parallel\left(\overleftrightarrow{I} + \left(\frac{1}{a_e} - 1\right)\mathbf{e}_z\mathbf{e}_z\right). \quad (4)$$

The size of $a_e$ or $a_m$ relative to 1 measures how large is the magnetic or electric anisotropy of the medium. Then, in the absence of external currents the plane-wave solution of Maxwell's equations for the electric field, $\mathbf{E} = \mathrm{Re}\left[\mathbf{E}_0 e^{i(\mathbf{k}\cdot\mathbf{r}-\omega t)}\right]$, is given by

$$\left[-\mathbf{k}\mathbf{k} + k^2\overleftrightarrow{I} - \mu_\parallel\omega^2\overleftrightarrow{\varepsilon} + (1-a_m)(\mathbf{k}\times\mathbf{e}_z)(\mathbf{k}\times\mathbf{e}_z)\right]\cdot\mathbf{E} = \mathbf{0}. \quad (5)$$

The solution of this equation, for finite $\mathbf{E}$, requires the determinant of the dyadic within the square brackets to vanish. This yields the dispersion relations of the electromagnetic modes in the system. In this case one finds that there are two bulk modes, whose dispersion relation can be written as

$$k_\alpha^2 = k_0^2 n_\parallel^2 + (1-a_\alpha)k_{\alpha_x}^2, \quad (6)$$

where $k_0 = \omega/c$, $n_\parallel = \sqrt{\varepsilon_\parallel\mu_\parallel/\varepsilon_0\mu_0}$, the sub-index $\alpha = m, e$ denotes the type of mode. Here we assume that the vectors $\mathbf{k}_\alpha$ lie on the $xz$ plane, and $k_{\alpha_x}$ denotes their $x$-component, while $k_\alpha$ denotes their magnitude. We use SI units, thus $\varepsilon_0$ and $\mu_0$ have their usual meaning. The modes will be self-propagating if $k_\alpha$ is real, while for $k_a^2<0$ the modes will be evanescent. Note that for $n_\parallel^2>0$, $\varepsilon_\parallel$ and $\mu_\parallel$ with the same sign and $a_\alpha<0$, the mode will be self-propagating. This means that there are self-propagating $e$ or $m$ bulk modes with only $\varepsilon_\perp<0$ or $\mu_\perp<0$, respectively. By calculating the eigenvectors in Eq. (5), one can see that if $a_e \neq a_m$ the polarisation of modes $e$ and $m$ is orthogonal. Specifically, the electric field for the mode with wavenumber $k=k_e$ lies in the $xz$ plane, while the mode with wavenumber $k=k_m$ lies along the $y$ direction. On the other hand, for $a_e=a_m$, there is only one possible mode and the electric field can have components both in the $xz$ plane and along the $y$ direction. It can also be shown that within this material there are induced charges in the bulk, given by $\rho_{ind} = (1+a_e^{-1})\varepsilon_0 k_z E_{0_z}$. This means that the $e$ mode is, in general, non-transverse. Obviously, when there is no anisotropy ($a_e=1$), is no induced charge density and the mode is transverse. There is an analogous behaviour for $\mathbf{H}$. For brevity in the notation, from now on we will call $\mathbf{A}_e$ to $\mathbf{E}_e$ and $\mathbf{A}_m$ to $\mathbf{H}_m$. We now calculate the angle $\phi_\alpha$ between $\mathbf{k}_\alpha$ and $\mathbf{A}_\alpha$ as a function of the angle $\Theta_\alpha$ formed by $\mathbf{k}_\alpha$ and the optical axis:

$$\cos\phi_\alpha(\Theta_\alpha; a_\alpha) = \frac{(1-a_\alpha)\mathrm{sgn}(\alpha_\parallel)\sin 2\Theta_\alpha}{2\sqrt{1-(1-a_\alpha)^2\sin^2\Theta_\alpha}}, \quad (7)$$

where $\alpha_\parallel$ and $\alpha_\perp$ denote $\varepsilon_\parallel$ and $\varepsilon_\perp$ when $\alpha=e$, and $\mu_\parallel$ and $\mu_\perp$ when $\alpha=m$. Note that this angle is independent of $n_\parallel$ and depends only on the anisotropy parameter $a_\alpha$ and the sign of $\alpha_\perp$. Also, one can show that under the change $a_\alpha \to 1/a_\alpha$ one gets $\cos\phi_\alpha(\pi/2-\Theta_\alpha; 1/a_\alpha) = -\mathrm{sgn}(\alpha_\perp)\cos\phi_\alpha(\Theta_\alpha; a_\alpha)$. This symmetry property is displayed in Fig. 1, where we plot $\phi_\alpha$ as a function of $\Theta_\alpha$ for different values of $a_\alpha$. One can see that for $\mathbf{k}_\alpha$ along the optical axis ($\Theta=0$) or perpendicular to it ($\Theta=\pi/2$) the angle $\phi_\alpha$ is always $\pi/2$, thus in this case the vectors $\mathbf{k}$, $\mathbf{E}$ and $\mathbf{H}$ are perpendicular to each other forming an orthogonal triad. For $0<a_\alpha<1$, the angle $\phi_\alpha$ is larger than $\pi/2$, attaining a maximum value (close to $\pi$), the smaller the value of $a_\alpha$. But for $a_\alpha>1$, the angle $\phi_\alpha$ becomes smaller than $\pi/2$ attaining a minimum value (close to 0), the larger the value of $a_\alpha$. For $a_\alpha<0$, the angle $\phi_\alpha$ is always larger than $\pi/2$ with a specular symmetry about $\Theta_\alpha = \pi/4$. One can see that for any value of $a_\alpha<0$, $\phi_\alpha$ always attains the value of $\pi$, in this case $\mathbf{A}_\alpha$ lies anti-parallel to $\mathbf{k}_\alpha$. Obviously, according to Maxwells equations, when this happens, the field $\mathbf{A}_\alpha$ vanishes. Naturally, the dynamics of the mode depends on the size of these angles, and one can see at once from Eq. (7) and the symmetry properties mentioned above, that the qualitative behaviour of a mode depends strongly on the sign of $a_\alpha$, which has necessarily a strong influence on the optical properties of this metamaterial.

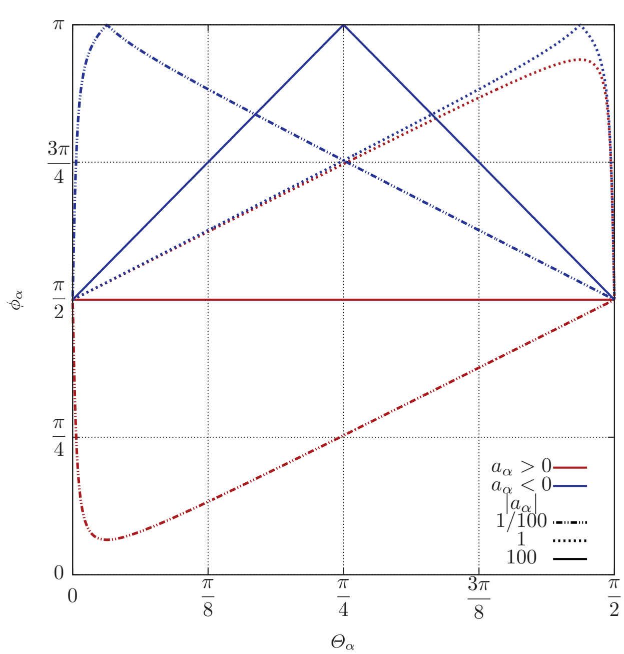


**Figure 1** (online colour at: www.pss-b.com) Angle between $\mathbf{k}_\alpha$ and $\mathbf{A}_\alpha$ as a function of $\Theta_\alpha$, for different values of $a_\alpha$.

Another important issue in the study of these modes is the way in which they transport energy; thus we calculate the Poynting vector $\mathbf{S}=\mathbf{E}\times\mathbf{H}$ associated to them. After averaging the cross product of the oscillating fields over time, one gets

$$\mathbf{S}_\alpha = \mathbf{A}^2_{\overline{\alpha}0}\frac{\mathbf{k}_\alpha + (a_\alpha - 1)k_{\alpha_x}\mathbf{e}_x}{2\alpha_\parallel\omega} = \frac{\mathbf{A}^2_{\overline{\alpha}0}}{2\omega}\left(\frac{k_{\alpha_x}}{\alpha_\perp}, 0, \frac{k_{\alpha_z}}{\alpha_\parallel}\right), \tag{8}$$

here $\overline{\alpha} = e, m$ if $\alpha = m, e$. It can readily be seen that, in each mode, the relative orientation between the Poynting vector $\mathbf{S}_\alpha$ and the wavevector $\mathbf{k}_\alpha$ can attain a wide range of values depending on the size and sign of the anisotropic response functions $\varepsilon_\parallel$, $\varepsilon_\perp$, $\mu_\parallel$ and $\mu_\perp$. This could have been already guessed by the wide range of values that $\phi_\alpha$ can reach. It can also be readily seen that the projection of $\mathbf{S}_\alpha$ on $\mathbf{k}_\alpha$ is proportional to $k_0^2 n_\parallel^2/\alpha_\parallel$, thus the sign of $\mathbf{S}_\alpha\cdot\mathbf{k}_\alpha$ is given by the sign of $\alpha_\parallel$ for mode $\overline{\alpha}$.

**3 Refraction** Here we consider a flat interface between a non-dissipative, isotropic medium with index of refraction $n_1 = \sqrt{\varepsilon_1\mu_1}$ and the anisotropic metamaterial. The interface lies perpendicular to the optical axis (at $z=0$) and a plane wave with wavevector $\mathbf{k}_1$ and $k_1 = k_0 n_1$, is incident at an angle $\theta_i$ from the isotropic medium. The setting of boundary conditions for the electric and magnetic fields requires

$$k_{1_x} = k_0 n_1 \sin\theta_i = k_{e_x} = k_{m_x} \equiv k_x. \tag{9}$$

A condition usually known as Snell's law. Therefore, in the presence of the interface, the dispersion relations for the transmitted or refracted electromagnetic modes in the anisotropic system are obtained by substituting Eq. (9) into Eq. (6), to yield

$$k_\alpha^2 = k_0^2\left[n_\parallel^2 + (1 - a_\alpha)n_1^2\sin\theta_i^2\right], \tag{10}$$

which looks like the dispersion relation in the bulk but with $k_x$ fixed by Snell's law.

**3.1 Refraction of the wavevector** By Snell's law $k_{1_x} = k_{\alpha_x} \equiv k_x$, but $k_1 \neq k_\alpha$, thus for each mode $\alpha$ there is an angle of refraction of the wavevector $\mathbf{k}_\alpha$ given by $\sin\Theta_\alpha = k_x/k_\alpha$, that can be written in a form similar to the usual Snell's law for isotropic media, as

$$N_\alpha(\theta_i)\sin\Theta_\alpha = \sin\theta_i, \tag{11}$$

where

$$N_\alpha(\theta_i) = \sqrt{n^2 + (1 - a_\alpha)\sin^2\theta_i}, \tag{12}$$

plays the role of an 'operative' relative index of refraction for mode $\alpha$, which depends not only on the values of the anisotropic components of the response functions but also on the angle of incidence. Here $n \equiv n_\parallel/n_1$. In case of normal incidence $\theta_i = 0$, one can immediately see from Eqs. (10) and (12), that only one mode is excited with wavevector $k = k_0 n_\parallel$ and $N_\alpha(0) = n$. For $\theta_i > 0$ both modes, $e$ and $m$, might be excited in the metamaterial, and they will be propagating whenever $|\sin\Theta_\alpha| \leq 1$ in Eq. (11), that is when $\Theta_\alpha$ is a real quantity. On the contrary, when $|\sin\Theta_\alpha| > 1$, we say that there is no refraction and this means that the excited $\alpha$ mode is evanescent.

One can immediately see in Eqs. (11) and (12), that the angle of refraction for each mode is an increasing function of the angle of incidence $\theta_i$ when $n^2 > 0$ and decreasing when $n^2 < 0$. The angle $\Theta_\alpha$ attains the value $\pi/2$ when the angle of incidence is equal to

$$\theta_{c_\alpha} = \arcsin\left(\frac{n}{\sqrt{a_\alpha}}\right), \tag{13}$$

which is called the critical angle. Thus, when $n^2 > 0$, the angle of refraction $\Theta_\alpha$ increases from 0, at normal incidence, up to $\pi/2$ at $\theta_i = \theta_{c_\alpha}$; when $n^2 < 0$, the behaviour of refraction is reversed, that is there is no refraction for normal incidence up to $\theta_i = \theta_{c_\alpha}$, where $\Theta_\alpha$ decreases from $\pi/2$ down to $\arcsin\left(1/\sqrt{1 + n^2 - a_\alpha}\right)$ at $\theta_i = \pi/2$.

In order for $\theta_{c_\alpha}$ to be a real number between 0 and $\pi/2$, when $n^2 > 0$, $a_\alpha$ should be a positive number between 0 and $n^2$; but when $n^2 < 0$, $a_\alpha$ should be a negative number smaller than $n^2$. If neither of these conditions is satisfied, there will not be a critical angle. In case $n^2 < 0$ and $a_\alpha > 0$, there would be no refraction at any angle of incidence and the system will behave as a perfect mirror, as we will show below.

It can also be seen from Eq. (12), that for $a_\alpha/n^2 \ll 0$, the operative index of refraction goes as $1/\sqrt{a_\alpha}\sin\theta_i$, for sufficiently large $\theta_i$. When this is inserted on Eq. (11), it gives an angle $\Theta_\alpha = \arcsin\left(1/\sqrt{a_\alpha}\right)$, independent of the angle of incidence. We illustrate this and the other previously stated properties in Figs. 2–4.

We now calculate, in a similar way, the refraction law for the wavevector in the inverse case, that is when the wave is incident from the anisotropic medium towards the isotropic one, assuming that the wavevector, the normal to the interface and the optical axis, lie all three on a plane, and that the last two form an angle $\gamma$ with respect to each other. Then we get

$$\sqrt{1 + (a_\alpha - 1)\sin^2\Theta_\alpha}\sin\theta_r = n\sin(\Theta_\alpha - \gamma). \tag{14}$$

Again, $\Theta_\alpha$ is the angle formed by the wavevector and the optical axis, and $\theta_r$ is the angle of refraction.

**3.2 Refraction of the Poynting vector** The actual angle of refraction that one detects and measures in the laboratory is the refraction of the flux of electromagnetic energy, that is the refraction of the Poynting vector. In dealing with the refraction of the Poynting vector one has to take into account the polarisation of the incident wave. It can be easily shown that when the interface is perpendicular to the optical axis, the polarisation of the incident wave is preserved in the transmitted (refracted) wave when the

 

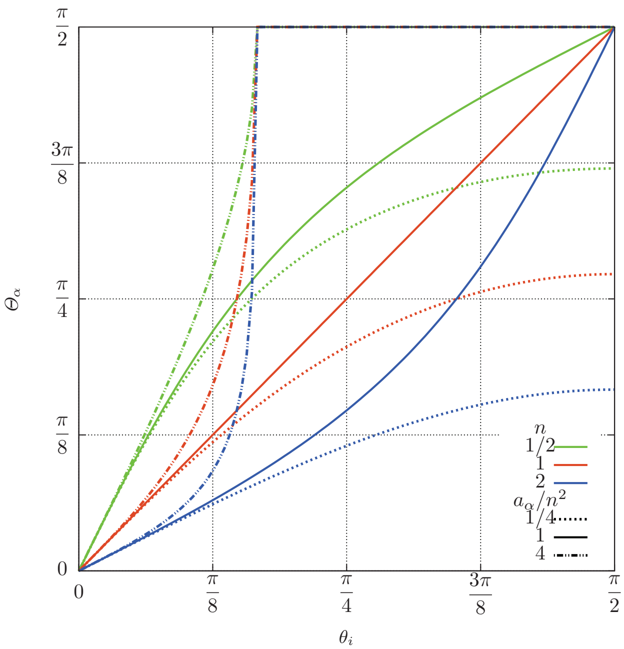


**Figure 2** (online colour at: www.pss-b.com) Angle between $\mathbf{k}_\alpha$ and the normal to the interface as a function of the angle of incidence, for $n^2>0$ and $a_\alpha>0$, for different values of $n^2$ (in colors), and $a_\alpha$ (in line styles) relative to $n^2$.

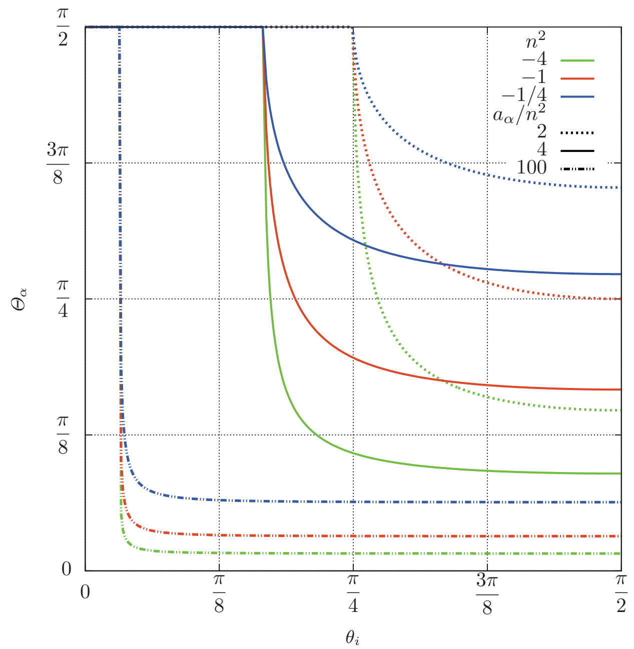


**Figure 4** (online colour at: www.pss-b.com) Angle between $\mathbf{k}_\alpha$ and the normal to the interface as a function of the angle of incidence, for $n^2<0$ and $a_\alpha<n^2$, for different values of $n^2$ (in colors), and $a_\alpha$ (in line styles) relative to $n^2$.

incident wave has either $s$ or $p$ polarisation. Let us recall that the electric field in $s$ polarisation, and the magnetic field in $p$ polarisation, are perpendicular to the plane of incidence ($xz$ plane). In $s$ polarisation the $m$ mode is excited while

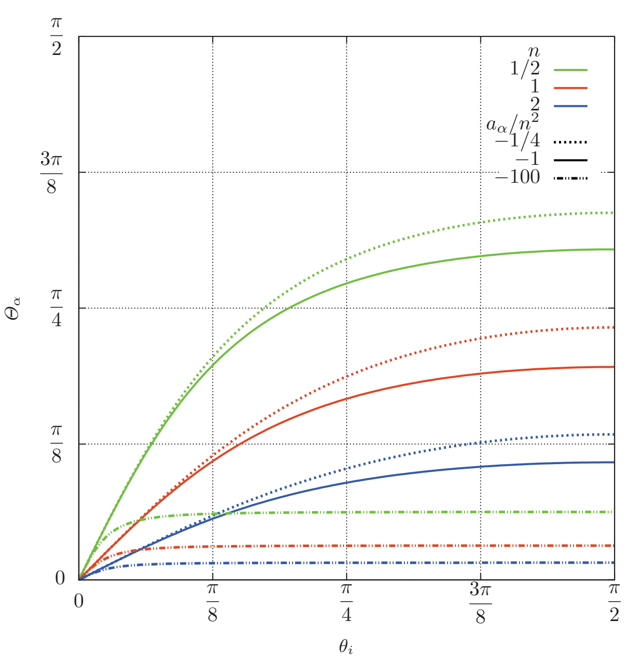


**Figure 3** (online colour at: www.pss-b.com) Angle between $\mathbf{k}_\alpha$ and the normal to the interface as a function of the angle of incidence, for $n^2>0$ and $a_\alpha<0$, for different values of $n^2$ (in colors), and $a_\alpha$ (in line styles) relative to $n^2$.

in $p$ polarisation is the $e$ mode the one excited, but in both cases the Poynting vector of the refracted wave lies in the $xz$ plane, and is given by

$$\mathbf{S}_\alpha = \frac{A_{0_{\bar{\alpha}}}^2}{2\omega}\left(\frac{k_x}{\alpha_\perp}, 0, \frac{k_{\alpha_z}}{\alpha_\parallel}\right), \tag{15}$$

where $\mathbf{S}_e$ corresponds to $p$-polarisation, $\mathbf{S}_e \equiv \mathbf{S}_p$, while $\mathbf{S}_m$ to $s$-polarisation, $\mathbf{S}_m \equiv \mathbf{S}_s$. The angle of refraction is the angle between the Poynting vector and the $z$ axis, and it can be written, in a single expression, as

$$\sin\theta_\alpha = \frac{S_{\alpha_x}}{S_\alpha} = \frac{k_x}{\alpha_\perp\sqrt{\frac{k_x^2}{\alpha_\perp^2} + \frac{k_{\alpha_z}^2}{\alpha_\parallel^2}}}. \tag{16}$$

Here $\theta_m$ corresponds to the angle of refraction for $s$ polarisation, while $\theta_e$ corresponds to the one for $p$ polarisation. Note that there will be negative refraction for $\mu_\perp<0$ in $s$ polarisation and for $\varepsilon_\perp < 0$ in $p$ polarisation, as has been already stated in Ref. [5]. This can also be seen in a more general way by writing the Poynting vector as

$$\mathbf{S}_s = \mathbf{E}_\parallel \times \mathbf{H}_\perp + \mathbf{E}_\parallel \times \mathbf{H}_\parallel \tag{17}$$

and

$$\mathbf{S}_p = \mathbf{E}_\perp \times \mathbf{H}_\parallel + \mathbf{E}_\parallel \times \mathbf{H}_\parallel, \tag{18}$$

where the sub-index $\parallel$ and $\perp$ in vectors $\mathbf{E}$ and $\mathbf{H}$ denote parallel and perpendicular components to the interface. The first term in these expressions corresponds to $\mathbf{S}_\parallel$,

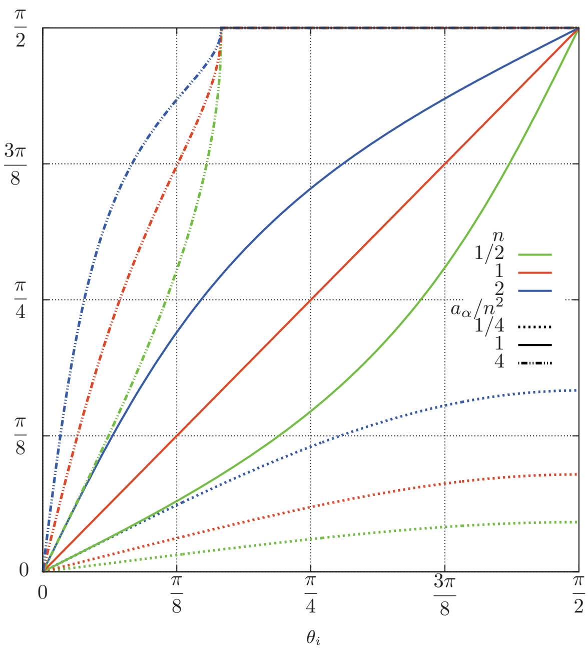


**Figure 5** (online colour at: www.pss-b.com) Angle of refraction as a function of the incidence angle, with the same material properties as in Fig. 2.

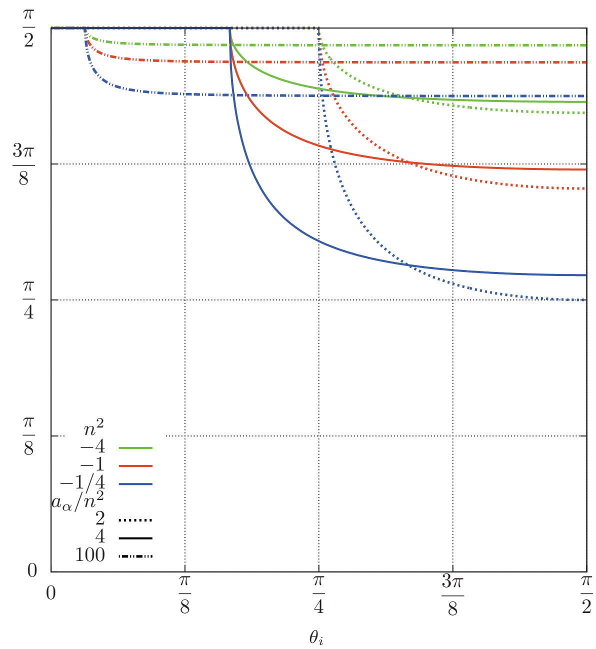


**Figure 7** (online colour at: www.pss-b.com) Angle of refraction as a function of the incidence angle, with the same material properties as in Fig. 4.

the parallel component of the Poynting vector; the second term corresponds to its perpendicular component, which is continuous at the interface, because the boundary conditions for the fields demand continuity of $\mathbf{E}_{\parallel}$ and $\mathbf{H}_{\parallel}$. Therefore, negative refraction will be possible if and only if $\mathbf{S}_{\parallel}$ changes of sign at the interface, and this requires that either $\mathbf{H}_{\perp}$ or $\mathbf{E}_{\perp}$ change sign. Since $\mathbf{B}_{\perp}$ and $\mathbf{D}_{\perp}$ are continuous at the interface, $\mathbf{H}_{\perp}$ and $\mathbf{E}_{\perp}$ can change sign if and only if $\mu_{\perp}<0$ or $\varepsilon_{\perp}<0$, respectively, and this becomes a necessary and sufficient condition for negative refraction. In contrast to the isotropic case, note that here negative refraction does not require a left-handed wave; furthermore, it requires only one response function to be negative, either $\mu_{\perp}$ or $\varepsilon_{\perp}$. This might become advantageous in the design of new metamaterials with negative refraction, as it has been pointed out, for example, in Ref. [6].

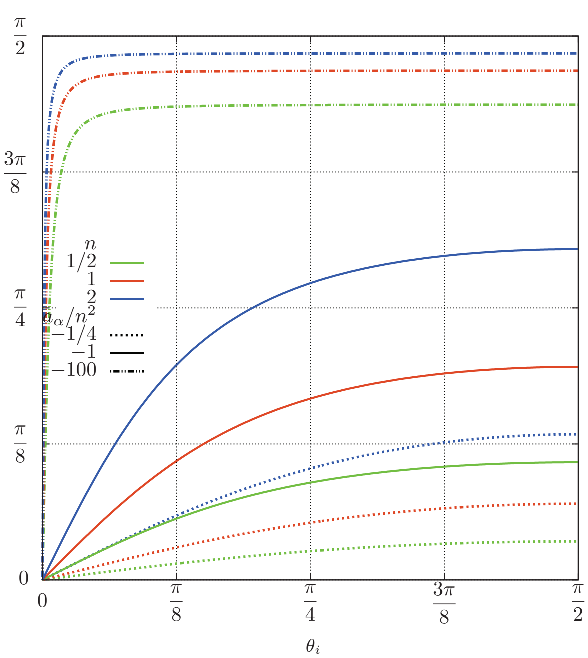


**Figure 6** (online colour at: www.pss-b.com) Angle of refraction as a function of the incidence angle, with the same material properties as in Fig. 3.

Now we use Eqs. (9)–(12) and (15) to write

$$\sin\theta_\alpha = \frac{|\alpha_{\parallel}|\sin\theta_i}{\alpha_{\perp}\sqrt{a_\alpha(a_\alpha-1)\sin^2\theta_i+n^2}}. \tag{19}$$

Here we see that there is also a critical angle, given by the same expression as in Eq. (13). One can also see that the angle changes only in sign when $\alpha_{\perp}<0$. In Figs. 5–7 we show the refraction angle as a function of the incidence angle, including curves where the angle of refraction remains practically constant.

### 3.3 The sign of S · k and negative refraction

Here we want to point out that, in contrast to the isotropic metamaterials negative refraction is not related with the sign of $\mathbf{S}\cdot\mathbf{k}$. Looking at Eq. (15) and realizing that $S_{\alpha_z}$ should be positive, for the energy to flow from the isotropic material towards the metamaterial, $k_{\alpha_z}$ and $\alpha_{\perp}$ should have the same sign. This sign is not determined by the dispersion relation of the modes given in Eq. (6), because this yields only the value of $k_{\alpha_z}^2$, thus we conclude that the sign of $\alpha_\parallel$ will determine the sign of $k_{\alpha_z}$. Now, being $\mathbf{S}_\alpha \cdot \mathbf{k}_\alpha = k_0^2 n_\parallel^2/\alpha_\parallel$ this projection has the sign of $\overline{\alpha}_\parallel$. But negative refraction, as it was mentioned above, is determined not by the sign of $\mathbf{S}_\alpha \cdot \mathbf{k}_\alpha$, but rather by the sign of $S_{\alpha_x}$, and this, as we have discussed, is determined by the sign of $\alpha_\perp$.

**4 Reflection** In this section we calculate the reflection and transmission amplitudes of the electric and magnetic fields upon the same flat interface as the one described in the treatment of refraction above. We also use the same coordinate system, thus the half space $z<0$ is occupied by an isotropic material with index of refraction $n_1>0$, while the half space $z>0$ is occupied by the anisotropic metamaterial. We define the reflection and transmission amplitudes, for $s$ polarisation as $r_s = E_s^r/E_s^i$ and $t_s = E_s^t/E_s^i$, and for $p$ polarisation as $r_p = H_p^r/H_p^i$, and $t_p = H_p^t/H_p^i$. Here the subscript $s$ and $p$ denote the polarisation while the superscripts $i$, $r$ and $t$ denote incident, reflected and transmitted field, respectively, and the quantities in the quotients mean amplitudes. Since in our case polarisation is preserved upon reflection and transmission, one can write

$$r_s = \frac{Z_s - Z_{1_s}}{Z_s + Z_{1_s}} \quad \text{and} \quad t_s = \frac{2Z_s}{Z_s + Z_{1_s}}, \tag{20}$$

$$r_p = \frac{Z_{1_p} - Z_p}{Z_{1_p} + Z_p} \quad \text{and} \quad t_p = \frac{2Z_{1_p}}{Z_{1_p} + Z_p}, \tag{21}$$

where $Z_s$ ($Z_p$) denotes the surface impedance of the anisotropic metamaterial for $s$ ($p$) polarisation, while $Z_{1_s}$ $\left(Z_{1_p}\right)$ denotes the corresponding quantity of the isotropic material. Here we have taken the convention that in $s$ ($p$) polarisation a + sign in $r_s$ ($r_p$) means that $E^i$ ($H^i$) does not change phase upon reflection. The surface impedance for $s$ ($p$) polarisation, in either material, is defined as $Z_{s(p)} = E_{\parallel_{s(p)}}\big/H_{\parallel_{s(p)}}$.

For the isotropic material, $Z_{1_s} = c\mu_1/n_1 \cos\theta_i$ and $Z_{1_p} = c\mu_1 \cos\theta_i/n_1$, where $c = \sqrt{\varepsilon_0\mu_0}$. For the anisotropic metamaterial, one gets

$$Z_s = c\frac{|\mu_\parallel|}{n_1 N_m(\theta_i)\cos\Theta_m} \quad \text{and} \quad Z_p = \frac{1}{c}\frac{n_1 N_e(\theta_i)\cos\Theta_e}{|\varepsilon_\parallel|}, \tag{22}$$

where, as mentioned above, the sign of $k_{\alpha_z}$ has been taken as the sign of $\alpha_\parallel$.

At normal incidence ($\theta_i = 0$), $\Theta_m = \Theta_e = 0$, and $Z_s = Z_p = \sqrt{\tilde{\mu}_\parallel/\tilde{\varepsilon}_\parallel}$, so the impedance matching condition to suppress reflection at normal incidence, will be given by $\tilde{\mu}_\parallel = \tilde{\varepsilon}_\parallel$, where the tilde above denotes a value relative to the one in the isotropic material, i.e. $\tilde{\mu}_\parallel = \mu_\parallel/\mu_1$, $\tilde{\varepsilon}_\parallel = \varepsilon_\parallel/\varepsilon_1$. But for $a_\alpha = n^2$ (i.e. $\theta_{c_\alpha} = \pi/2$), which means $\tilde{\mu}_\perp = 1/\tilde{\varepsilon}_\parallel$ for $\alpha = m$ and $\tilde{\mu}_\parallel = 1/\tilde{\varepsilon}_\perp$ for $\alpha = e$, one gets $Z_s = \sqrt{\mu_\parallel/\varepsilon_\parallel}/\cos\theta_i = Z_p$. Thus the reflection amplitude for both polarisations becomes

$$r = \frac{\sqrt{\tilde{\mu}_\parallel} - \sqrt{\tilde{\varepsilon}_\parallel}}{\sqrt{\tilde{\mu}_\parallel} + \sqrt{\tilde{\varepsilon}_\parallel}}, \tag{23}$$

independent of the angle of incidence. Furthermore, in the particular case in which we set $\tilde{\mu}_\parallel = \tilde{\varepsilon}_\parallel$ and $\tilde{\mu}_\perp = \tilde{\varepsilon}_\perp = 1/\tilde{\mu}_\parallel$, there will be no reflection at any angle of incidence for either polarisation. This is what is called: perfect impedance matching condition, and a slab made of a material fulfilling these conditions would be non-reflective [7].

We now turn to the calculation of the reflectance and transmittance. The reflectance has the usual form

$$R_\alpha = r_\alpha^2, \tag{24}$$

while the transmittance can be written in the form

$$T_\alpha = t_\alpha^2 \frac{N_\alpha(\theta_i)}{|\alpha_\parallel|}\frac{\cos\Theta_\alpha}{\cos\theta_i} \tag{25}$$

and they obey $R_\alpha + T_\alpha = 1$. From these expressions it can be readily seen that this material has a Brewster angle given by

$$\theta_{B_\alpha} = \arcsin\sqrt{\frac{n^2 - \tilde{a}_\parallel^2}{a_\alpha - \tilde{a}_\parallel^2}}, \tag{26}$$

where $\tilde{a}_\parallel$ is $\alpha_\parallel/\varepsilon_1$ if $\alpha = e$ and $\alpha_\parallel/\mu_1$ if $\alpha = m$. In particular, this implies that propagating modes with $n^2<0$ always have a Brewster angle. In Figs. 8–10 we plot the reflectance as a

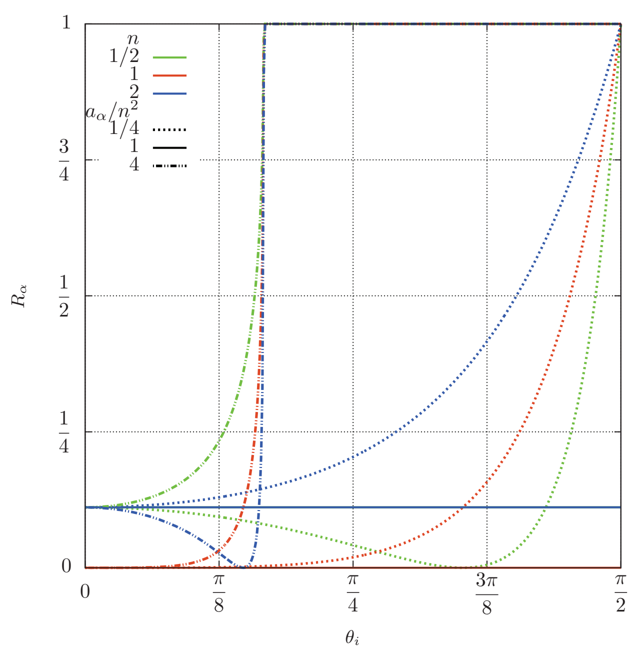


**Figure 8** (online colour at: www.pss-b.com) Reflectance of the $\alpha$ mode as a function of the incidence angle for the same material properties as in Fig. 2, with $\alpha_\parallel = 1$.

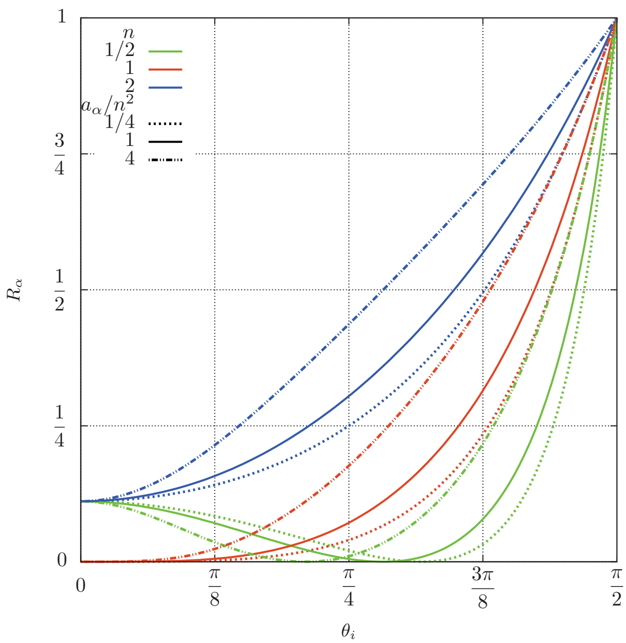


**Figure 9** (online colour at: www.pss-b.com) Reflectance of the $\alpha$ mode as a function of the incidence angle for the same material properties as in Fig. 3, with $\alpha_\parallel = 1$.

function of several parameters. In Fig. 8 we can see, in particular, constant-reflectance curves (including one with zero reflectance) as well as total reflection after the critical angle. In Fig. 9 the critical angle does not exist, since the values of $a_\alpha$ where switched to their negatives with respect to the ones in Fig. 8. In Fig. 10 we can appreciate that all

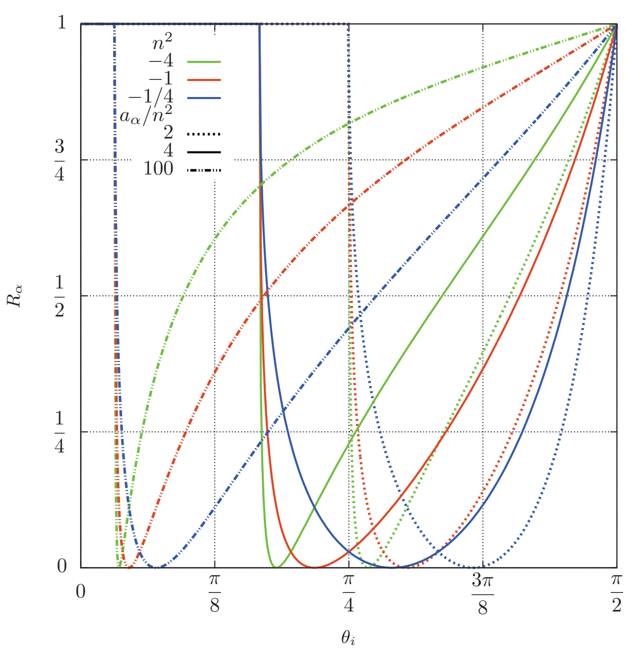


**Figure 10** (online colour at: www.pss-b.com) Reflectance of the $\alpha$ mode as a function of the incidence angle for the same material properties as in Fig. 4, with $\alpha_\parallel = 1$.

curves have a Brewster angle, as it can be seen from Eq. (26), and total reflection is obtained before the critical angle, which always exists. In all graphics, the reflectance at normal incidence depends only on $n$ and $\alpha_\parallel$.

**5 Diffuse light collimator** Here we take advantage, as noted in Section 3, of the near-constant refraction angle behaviour of the anisotropic metamaterial, in the limit $a_\alpha \to -\infty$, to propose a design of a diffuse-light collimator.

Let us consider an arrangement like the one in Fig. 11. The device to the left is made of an anisotropic metamaterial with $\overleftrightarrow{\varepsilon} = \overleftrightarrow{\mu}$ and $a_\alpha \ll 0$. Light, incident from the left in the $xz$ plane, gets refracted to an angle close to $\pi/2$, and has a wavevector with an angle, relative to the optical axis, close to $\arcsin\left(n/\sqrt{a_\alpha}\right)$. The device has an angle such that the wavevector is closely aligned to the normal to the second surface, and therefore suffers little deviation from it. After this, light gets to a second, isotropic device, with an index of refraction $n'$ relative to the surrounding medium, which straightens it towards the $z$ direction.

Rotating this arrangement over the $z$ axis, we get two cones, one anisotropic with its optical axis coinciding with the cone axis, and one isotropic. When light strikes the left surface of such device in arbitrary direction, the incidence plane always contains the optical axis, as we have supposed in all this study, so all refracted rays will behave in the same way. Therefore, diffuse light incident on this device would be collimated.

To estimate how much light gets collimated, we established the following criterion: we set a desired angular tolerance $\Delta\theta$ for collimation. Assuming that the intensity of incident light is uniformly distributed over all angles, we calculate the fraction of power that gets collimated up to a $\Delta\theta$ degree with respect to the $z$ axis, relative to the incident power. We call this fraction $F$. Numerical calculations of this number can be seen in Fig. 12, plotted as a function of $a_\alpha$ for different values of $n$ and $n'$. We can see that for certain modest values of $n$, $n'$ and $a_\alpha$, we get fractions of power close

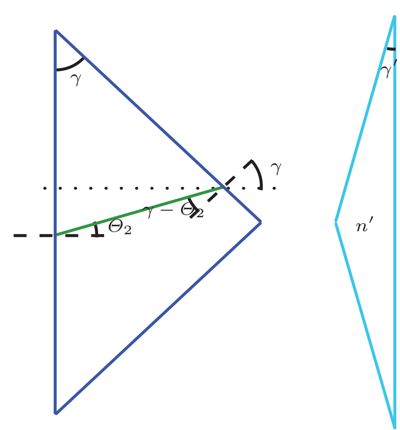


**Figure 11** (online colour at: www.pss-b.com) Schematic view of the collimator. To the left, an anisotropic metamaterial with $a_\alpha \ll 0$. To the right, an isotropic material with index of refraction $n'$ relative to the surrounding medium.

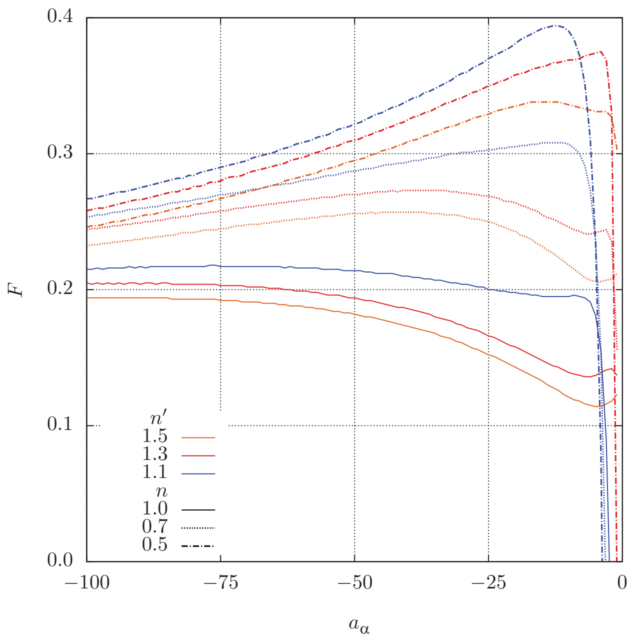


**Figure 12** (online colour at: www.pss-b.com) Fraction of power collimated to $1^\circ$, for different values of $n$ and $n'$, with $\alpha_\| = -1$, as a function of $a_\alpha$, assuming equal permittivity and permeability tensors.

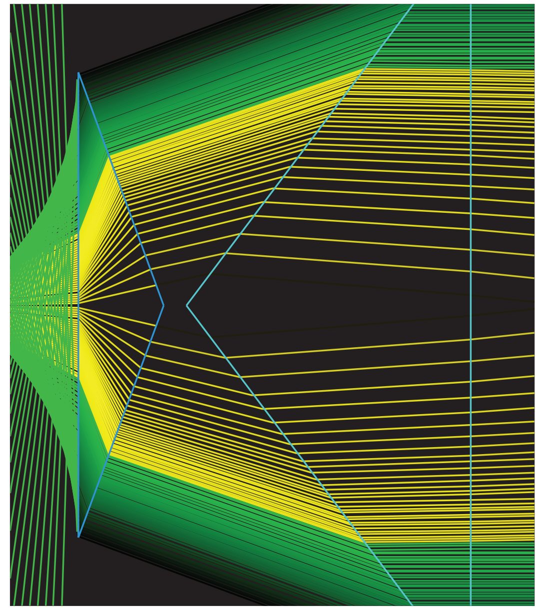

**Figure 14** (online colour at: www.pss-b.com) The analogous diagram of previous figure when using the values $a_\alpha = -7$, $n = 0.5$, $n' = 21.4$, $\alpha_\| = -1$ for which we get $F \approx 0.19$.

to 0.4 collimated to $1^\circ$. In Figs. 13 and 14 we can see ray diagrams of the collimator, for two particular cases, showing the intensity of rays and distinguishing the collimated rays from the non-collimated ones. We may even relax the condition $\overleftrightarrow{\varepsilon} = \overleftrightarrow{\mu}$: it would be sufficient to have $a_e = a_m$ for

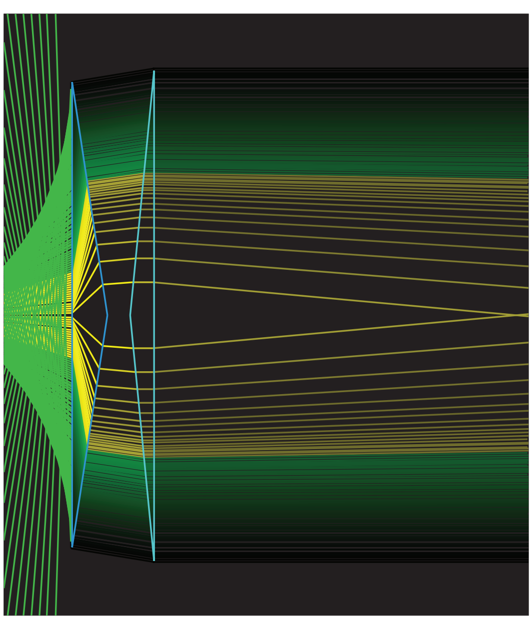

**Figure 13** (online colour at: www.pss-b.com) Ray diagram of the collimator for $a_\alpha = -41$, $n = 0.70$, $n' = 2.5$, $\alpha_\| = -1$. Green denotes the rays collimated to a precision of $1^\circ$, and yellow all other rays. Here $F \approx 0.39$. Rays are traced with their respective intensities.

the angles to behave this way, although different intensities would be transmitted for each polarisation. Even if we do not have $a_e = a_m$, the analysis would be true, on the average, for half of the light, assuming that the incident light is polarised half $s$ and half $p$.

Do the properties imposed over the anisotropic material, as required by this study, can be obtained in practice? For instance, relatively simple metamaterials like layered structures [8], or metallic nanowires [9] have been proposed, and extreme values of anisotropies have been reported [9–11], including natural materials [12]. Some of them even have the extreme important condition of having low dissipation [13]. All of them exhibit negative effective components of $\overleftrightarrow{\varepsilon}$ and $\overleftrightarrow{\mu}$ for certain frequency ranges that even reach the THz range [10].

**6 Conclusions** We derived the dispersion relations of the two self-propagating modes in arbitrary anisotropic uniaxial metamaterial and studied the light refraction and reflection characteristics of a flat interface between this anisotropic metamaterial and an isotropic one. We confirmed that having a negative perpendicular component of the tensorial optical response $\overleftrightarrow{\varepsilon}$ and $\overleftrightarrow{\mu}$, is an equivalent condition of having negative refraction of the corresponding mode. We also, (i) show that there exists a limit in the optical parameters of the metamaterial at which refraction angles are approximately independent of the angle of incidence, (ii) found that there can be propagating waves with a reverse critical angle behaviour when the signs of the parallel components of the response tensors are opposite, (iii) found the conditions for the existence of this angle, as well as the Brewster angle and (iv) found conditions for constructing materials with constant reflectance, which can be in particular non-reflective. Finally, we used these results to propose the design of a diffuse-light collimator with a high efficiency and simple geometry.

## References

[1] L. D. Landau and E. M. Lifshitz, Electrodynamics of Continuous Media (Pergamon Press, Oxford, 1984).
[2] V. G. Veselago, Sov. Phys. Uspekhi **10**, 509 (1968).
[3] J. B. Pendry et al., IEEE Trans. Microwave Theory Tech. **47**(11), 2075 (1999).
[4] D. R. Smith et al., Phys. Rev. Lett. **90**, 077405 (2003).
[5] L. Hu and S. T. Chui, Phys. Rev. B **66**, 085108 (2002).
[6] J. Elser et al., Appl. Phys. Lett. **89**, 261102 (2006).
[7] U. Leonhardt et al., New J. Phys. **8**, 247. (2006).
[8] Y. Huang et al., J. Appl. Phys. **105**, 013532 (2009).
[9] A. Fang et al., Phys. Rev. B **79**, 245127 (2009).
[10] S. Wang et al., Phys. Lett. **97**, 181902 (2010).
[11] T. Oates et al., Opt. Express **19**, 3 (2011).
[12] J. Sun et al., Appl. Phys. Lett. **98**, 101901 (2011).
[13] J. Sun et al., New J. Phys. **12**, 083020 (2010).